Ocean Engineering 55 (2012) 71–80

Contents lists available at SciVerse ScienceDirect

Ocean Engineering

journal homepage: www.elsevier.com/locate/oceaneng

A prediction method for squat in restricted and unrestricted rectangular fairways

Evert Lataire [a,*], Marc Vantorre [a], Guillaume Delefortrie [b]

[a] Ghent University, Maritime Technology Division, Technologiepark 904, 9052 Ghent, Belgium
[b] Flanders Hydraulics Research, Berchemlei 115, 2140 Antwerp, Belgium

ARTICLE INFO

Article history:
Received 23 November 2011
Accepted 1 July 2012
communicated by A.I. Incecik
Available online 18 August 2012

Keywords:
Squat
Shallow water hydrodynamics
Model tests
Mathematical model

ABSTRACT

The hydrodynamic behaviour of a vessel changes when sailing in shallow and/or confined water. The restricted space underneath and alongside a vessel has a noticeable influence on both the sinkage and trim of a vessel, also known as squat. To assess these influences an extensive model test program has been carried out in the *Towing Tank for Manoeuvres in Shallow Water* (cooperation *Flanders Hydraulics Research — Ghent University*) in Antwerp, Belgium with a scale model of the KVLCC2 Moeri tanker. This benchmark vessel was selected for its full hull form, to maximize the effects of the blockage.

To thoroughly investigate the influences of the blockage on the squat of the vessel, tests have been carried out at different water depths, widths of the canal section and forward speeds (2 up to 16 knots full scale whenever possible).

The squat observed during the model tests is compared with the squat predicted with a mathematical model based on mass conservation and the Bernoulli principle. The correlation between measured and modelled squat for each canal width for all tested speeds and water depths is very good, but shows a constant slope deviation. An improved model for the squat is proposed and takes into account the forward speed, propeller action, lateral position in the fairway, total width of the fairway and water depth.

1. Introduction

A sailing ship continuously displaces and accelerates a significant amount of water, which, according to the Bernoulli principle, results in a pressure drop around the vessel. The latter yields a vertical displacement characterized by values of the running sinkage at the forward and the aft perpendiculars, or alternatively, a mean running sinkage and trim. This phenomenon is commonly referred to as squat (Briggs et al., 2010). Principally, the ship does not undergo an increase of its draft or volume displacement, but the level of the free water surface around the vessel changes and, on average, drops. As a result, the ship translates vertically and rotates around its lateral axis.

Squat also occurs in deep and open water but is more pronounced in restricted or confined waters. Moreover, in deep and open water this phenomenon has no major consequences, while in more restricted waters the vessel can run aground. A decrease of the net underkeel clearance as a result of squat may also affect the ship's manoeuvrability dramatically, resulting in loss of control.

An accurate prediction of the squat that is valid in the complete range from deep and open waters up to narrow and shallow waterways (i.e., channels, canals, docks, locks) is therefore important, to avoid not only groundings but also manoeuvrability issues due to insufficient underkeel clearances. The aim of the present paper is to predict the squat (sinkage and trim) for a wide range of water depths and widths of a canal with rectangular cross section. The forward speed, lateral position of the vessel in the canal, propeller action and hull geometry are taken into account.

In June 2010 systematic model tests were carried out in the *Towing Tank for Manoeuvres in Shallow Water* (cooperation *Flanders Hydraulics Research — Ghent University*). The sinkage of a scale model of a very large crude carrier was measured, the lateral position and the forward speed of the model were varied systematically resulting in a database of about 400 different model tests.

The model test results are compared with the semi-empirical calculation method as published by Dand and Ferguson (1973). Based upon this theory a new mathematical model is proposed for the calculation of squat in any rectangular cross section, from a wide and deep fairway, up to underkeel clearances of only a few percent of the vessel's draft and widths of a fraction more than

* Corresponding author. Tel.: +32 92645557; fax: +32 92645843.
E-mail addresses: Evert.Lataire@UGent.be (E. Lataire), Marc.Vantorre@UGent.be (M. Vantorre), Guillaume.Delefortrie@mow.vlaanderen.be (G. Delefortrie).
URL: http://www.shallowwater.be (G. Delefortrie).

0029-8018/$ - see front matter
http://dx.doi.org/10.1016/j.oceaneng.2012.07.009

Nomenclature

A_C [m^2] Canal cross section area
A_M [m^2] Area of midship section
A_W [m^2] Waterplane area
$A(x)$ [m^2] Cross section area of the ship at longitudinal position x
$B(x)$ [m] Beam of the waterline at longitudinal position x
B [m] Beam of the ship
D [m] Propeller diameter
F_{NR} [N] Rudder normal force
F_{TR} [N] Rudder tangential force
Fr_h [dimensionless] Froude number (water depth dependant)
Fr_{crit} [dimensionless] Critical speed
g [m/s^2] Gravity of Earth
h [m] Water depth
I_L [m^4] Longitudinal moment of inertia
L_{PP} [m] Length between perpendiculars
K [Nm] Roll moment
M [Nm] Trim moment
m [dimensionless] Blockage
m_{crit} [dimensionless] Critical blockage
N [Nm] Yaw moment
n [rpm] Propeller rate
Q_P [Nm] Torque on the propeller shaft
R^2 [dimensionless] Coefficient of determination
Q_R [Nm] Torque on the rudder
T [m] Draft
t [m/m] Trim
T_P [N] Thrust of the propeller
V [m/s] Forward speed of the vessel
V_1 [m/s] Speed of the water in the disturbed cross section
V_{eq} [m/s] Equivalent forward speed
V_T [m/s] The axial speed in the flow field behind the propeller induced by the propeller
W [m] Width of the canal section
W_0 [m] Part of the model that takes into account the total width of the cross section
W_{eq} [m] Equivalent width of the canal section
W_y [m] Part of the model that takes into account the influence of the eccentric position in the rectangular canal
x [m] Longitudinal position from the aft perpendicular
X [N] Longitudinal force
y [m] Lateral position in the canal section
Y [Nm] Sway force
z [m] Sinkage
Z [N] Vertical force
δ [°] Rudder angle
$\delta V(x)$ [m/s] Speed difference between the disturbed and undisturbed flow
ξ_i [dimensionless] Coefficient of the mathematical model
γ [dimensionless] Tuck's formula
ζ [m] Decrease of the water level in the cross section
ρ [kg/m^3] Density
∇ [m^3] Displacement

Subscripts

$_A$ [dimensionless] At the aft perpendicular
$_{crit}$ [dimensionless] Critical speed
$_F$ [dimensionless] At the forward perpendicular
$_M$ [dimensionless] At midship
$_V$ [dimensionless] Running

the beam of the ship. The application range of the proposed model is restricted to channels with a rectangular cross section, and to vessels sailing without drift and parallel to the longitudinal channel boundaries.

2. State of the art

For years the combination of mean running sinkage z_{VM} and running trim t_V (or squat) has been investigated at different research institutes. Published scientific research on squat initiated with Constantine (1960) who discussed the different squat behaviour for subcritical, critical and supercritical vessel speeds and its theoretical relation with the blockage factor m (or the ratio between the midship section A_M and the cross section of the fairway A_C). Constantine's reflections were essentially based on a one-dimensional approach, assuming a constant return flow and a constant water level drop over a cross-section. Therefore, his results are only valid for waterways with limited width, and tend to zero for open (i.e., laterally unrestricted) water.

Tuck (1966) presented an analytical solution for squat of ships in open water. In the subcritical domain, he proved for laterally open water conditions of constant depth h that the sinkage and trim of a vessel sailing at a constant speed V is proportional to the parameter $\gamma(Fr_h)$ (all symbols are listed in the nomenclature):

$$\gamma(Fr_h)=\frac{Fr_h^2}{\sqrt{1-Fr_h^2}} \tag{1}$$

in which Fr_h represents the depth-related Froude number

$$Fr_h=\frac{V}{\sqrt{gh}} \tag{2}$$

Tuck's theory was later extended to dredged channels by Beck et al. (1975) with a matching of solutions between the deep and shallow regions of the cross section. Naghdi and Rubin (1984) solved Tuck's problem using a nonlinear steady-state solution of the differential equations of the theory of a thin ship while Cong and Hsiung (1991) combined the thin ship and flat ship theory to solve the same problem for transom stern ships.

Tuck's theory predicts infinite squat for the critical speed value $F_{nh}=1$. On the other hand, using methods based on the Bernoulli principle and conservation of mass as proposed by Constantine (1960), Dand and Ferguson (1973) and Gourlay (1999) give a blockage-dependent critical speed range instead of one particular critical speed value. In order to extend their theoretical developments towards random bottom conditions and waterways with large width, Dand and Ferguson (1973) and Gourlay (2000) relied upon experimental research. A correction for the effect of the propeller was proposed by Dand (1972). To cope with large or even infinite canal widths, Dand (1972) applied the effective width parameter $\overline{W}$ (Eq. (3)) introduced by Tuck (1967) that was based upon model tests in a section width from 7.5 to about 14 times the beam of the vessel.

$$\overline{W}=\frac{W}{L_{pp}}\sqrt{1-Fr_h^2} \tag{3}$$

Many empirical methods for estimation of ship squat have been published. It is not the authors' intention to give an exhaustive overview of these formulations, but only to mention the methods that explicitly account for the canal geometry. Führer and Römisch (1977) also proposed empirical formulae based on model tests to predict the squat for different cross section parameters of the fairway. Extensive model tests with 13 different ship models and three different canal geometries were carried out and analysed by Guliev (1971). Even though most of the conclusions still stand, Guliev's prediction method is used less as it is a graphical method.

More practical methods based on experimental research are presented by Barrass (1979), who also proposed an equivalent width taking into account the dimensions of the width of the fairway. However, the results obtained by Barrass (1979) were not validated by Seren et al. (1983).

More general overviews are presented in Dumas (1982), Millward (1990), PIANC (1997) Working Group 30 and Blaauw and Van der Knaap (1983). The latter extensively compared all methods published at the time with model tests and proposed the most suitable method for different situations. Jiang and Henn (2003) present a numerical method valid from subcritical to supercritical speed. An overview of slender body methods is presented in Gourlay (2008).

Besides measurements on model scale, interesting full-scale observations were carried out by Ankudinov et al. (2000), Stocks et al. (2004) and Härting et al. (2002, 2009) among others. Most discussions focus on ships sailing in open water or in rectangular shaped canals without drift angle or propulsion. In some cases the drift angle was considered, as by Von Bovet (1985), Martin and Puls (1986), de Koning Gans and Boonstra (2007) and Eloot et al. (2008). The squat when sailing in a muddy area is investigated by Sellmeijer and van Oortmerssen (1983), Vantorre and Coen (1988), Brossard et al. (1990), Doctors et al. (1996) and most recently by Delefortrie et al. (2010). For an exhaustive overview of publications and calculation methods related to the squat phenomenon, the reader can refer to Briggs et al. (2010).

3. Experimental program

3.1. Test facilities

All the test results discussed in the present paper are obtained by captive model tests carried out in the *Towing Tank for Manoeuvres in Shallow Water* (cooperation *Flanders Hydraulics Research — Ghent University*). The main dimensions of the empty towing tank are $88 \times 7 \times 0.5\ m^3$ (Van Kerkhove et al., 2009), but vertical walls parallel to the longitudinal tank walls were built into the tank to reduce the channel width over a length of 30 m. The tank is equipped with a planar motion carriage that allows both captive and free-running manoeuvring tests.

These model tests are carried out with a model that represents a Very Large Crude Carrier (VLCC) at scale 1/75. The geometric properties of bare hull, propeller and rudder of this vessel are made available and published via (SIMMAN, 2008). This specific model is known as the *KVLCC2 Moeri tanker* and often used as a benchmark vessel by towing tanks worldwide (Stern and Agdrup, 2008). The main properties of the vessel are summarized in Table 1 and the body plan is shown in Fig. 1.

During the test series the ship model was connected rigidly to the planar motion carriage of the towing tank. The ship model's trajectory was determined in the horizontal plane by the motion of the mechanism but the model was free in the vertical degrees of freedom allowing trim and sinkage.

During every test run the running sinkage of the model was measured at four discrete positions (fore/aft and port/starboard). Based upon these measurements the running sinkage at the forward perpendicular z_{VF} and at the aft perpendicular z_{VA} was derived. Note that the model was not free to roll, the starboard and port measurements should therefore be equal. In addition to the sinkage, forces and moments on hull, propeller and rudder, as listed in Table 2, were also measured.

Table 1
Main properties of VLCC ship model.

Ship model characteristic	Full scale	Model	Unit
Scale	1	75	–
L_{PP}	320.0	4.267	[m]
B	58.0	0.773	[m]
T_F	20.8	0.277	[m]
T_A	20.8	0.277	[m]
∇	312622	0.741	[m^3]

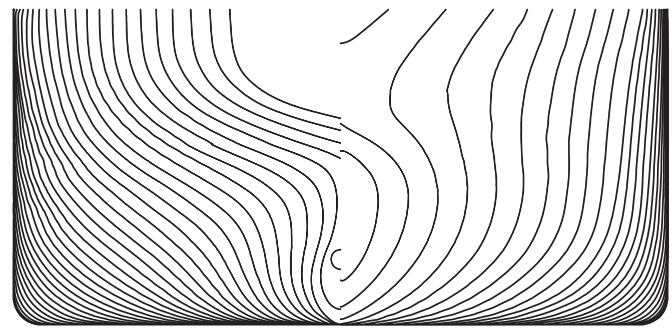

Fig. 1. Body plan of the KVLCC2 including the water line at the tested draft (design draft).

Table 2
Measured forces, moments and vertical translations on the ship model.

Ship model characteristic	Symbol	Unit
Running sinkage at the FP and AP	z_{VF}, z_{VA}	[m]
Longitudinal force	X	[N]
Sway force	Y	[N]
Yaw moment	N	[Nm]
Roll moment	K	[Nm]
Propeller thrust	T_P	[N]
Propeller torque	Q_P	[Nm]
Propeller rate	n	[rpm]
Rudder normal force	F_{NR}	[N]
Rudder tangential force	F_{TR}	[N]
Rudder torque	Q_R	[Nm]
Rudder angle	δ_R	[deg]

3.2. Test parameters

The ship model was towed at a constant forward speed along different lateral positions in the rectangular canal with the velocity vector always parallel to the longitudinal walls of the canal (Fig. 2). The canal was open at the inlet and outlet so water from the towing tank could flow in and out the actual canal section during a test run. The width W of the canal section was varied from only 1.05 times the ship's beam B up to the entire width of the towing tank (7.00 m or 9.05 B). Also a range of water depths was tested from 1.05 T to 1.50 T, the latter being close to the maximum possible water depth in this shallow water towing tank (Fig. 3). The blockage factor m (or the ratio between the midship section A_M and the cross section of the fairway A_C) is summarized in Table 3. In the narrowest canal section, the acceleration of the ship model was initiated in the test section

Fig. 2. The KVLCC2 towed in the most confined canal section (W=1.05 B).

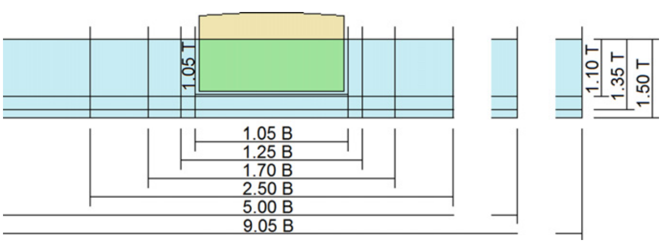

Fig. 3. Overview of all tested cross sections.

Table 3
Overview of tested blockage factors m.

	Canal width W					
Water depth h	**1.05 B**	**1.25 B**	**1.70 B**	**2.50 B**	**5.00 B**	**9.05 B**
1.05 T	0.91	-	-	-	-	-
1.10 T	0.86	0.73	0.53	0.36	0.18	0.10
1.35 T	0.70	0.59	0.43	0.30	0.15	0.08
1.50 T	0.63	0.53	0.39	0.27	0.13	0.07

while for all other canal sections the acceleration started with the bow of the model at the entrance of the section. The deceleration started when the vessel was out of the test section for all canal widths. For all model tests it is manually checked that only the running sinkage at the steady state condition was used after all transitional phenomena induced by the acceleration were damped, and before the deceleration or the end of the canal section was reached. This steady-state interval was different depending of the test condition but the model covered a distance,

Table 4
Distance between the longitudinal centreline of the model and centreline of the fairway y [m] in model scale.

	Canal width W [m]					
y_{wall} [m]	**1.05 B**	**1.25 B**	**1.70 B**	**2.50 B**	**5.00 B**	**9.05 B**
0.020	-	0.077	0.251	0.560	1.526	-
0.050	-	0.047	0.221	0.530	1.496	-
B/4	-	-	0.077	0.386	1.352	-
B/2	-	-	-	0.193	1.159	-
B	-	-	-	-	0.773	2.340
2 B	-	-	-	-	-	1.567
3 B	-	-	-	-	-	0.794
Centreline or $\frac{W-B}{2}$	0.000	0.000	0.000	0.000	0.000	0.000

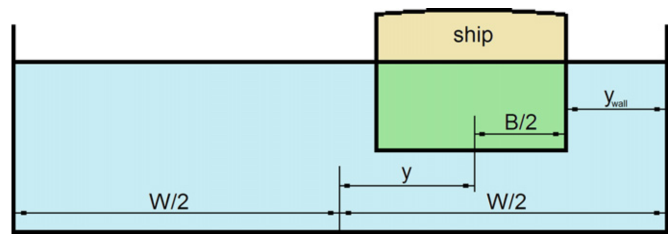

Fig. 4. Graphical interpretation of the lateral position of the vessel in the cross section of the model fairway.

at a constant forward speed, of at least two ship lengths and the used measurements end before the bow was as close as one ship length from the end of the canal.

All tested lateral positions y, expressing the distance between the centreline of the vessel and centreline of the fairway, for all canal widths are summarized (in model scale) in Table 4. The distance y_{wall} is defined as:

$$y_{wall} = \frac{W}{2} - \frac{B}{2} - y \tag{4}$$

Whenever possible the lateral position of the vessel (Fig. 4) in the canal was varied systematically from sailing at a distance as close as 0.020 m (1.5 m full scale) between the ship's port side and the wall of the test canal up to sailing at the centreline of the canal.

The forward speed of the towed VLCC model has been varied from 0.2 knots up to 16.0 knots full scale, the higher speeds being only feasible in the deeper and wider canals. An overview of the tested forward speeds in each water depth — canal width combination is given in Fig. 5.

The propeller rate n of the model at each tested forward speed was always at the self propulsion point in open water i.e., without the influence of the water depth or width of the canal. The tests carried out with the entire width of the towing tank available (W=9.05 B) were also carried out with a fixed propeller (n=0).

4. Empirical method by Dand and Ferguson

4.1. Principle

Dand and Ferguson (1973) proposed a semi-empirical theory to calculate the squat as a combination of mean sinkage and trim based on the mass conservation law and the Bernoulli principle. Hereafter, Dand and Ferguson (1973) will be referred to as D&F. This theory takes into account the ship's beam $B(x)$ on the waterline at a longitudinal position x, the cross-sectional area $A(x)$ and the longitudinal distribution of these areas. It supposes

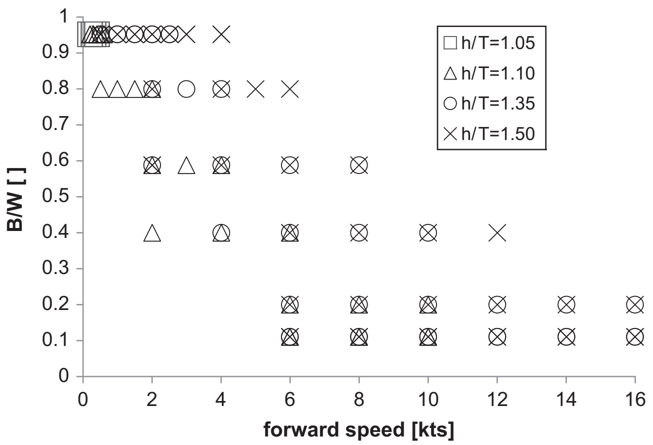

Fig. 5. Overview of tested forward speeds for all canal width — water depth combinations.

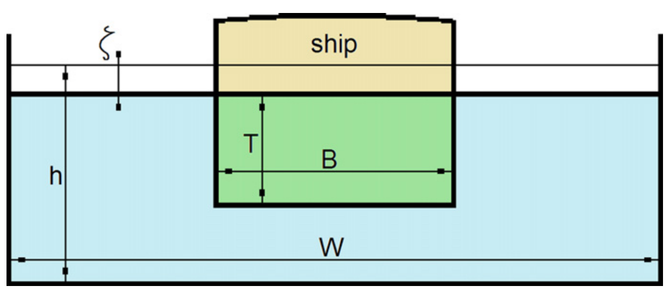

Fig. 6. The main variables in a cross section with the vessel on the centreline of the fairway, with the decrease ζ of the water level.

that the vessel sails at a constant speed V in a waterway with rectangular cross section A_C with a constant water depth h (at rest) and width W. When the vessel sails in open water an equivalent width of the section is used and a compensation for the propeller action on the trim of the vessel is proposed. However, these last three parameters are not included initially in the analyses. They are included later with the suggested modifications to the D&F method.

When the vessel sails with a speed over ground V on a straight course along the centreline of this rectangular fairway, a return flow will be initiated at each section (x), so that the velocity of the water at the entire section is increased by $\delta V(x)$. Because of the increased water speed along this section, the pressure will decrease (Bernoulli principle), causing a decrease of the water level over a vertical distance $\zeta(x)$ proportional to the pressure drop (Fig. 6).

The conservation of mass can be written as

$$A_C V = V_1(x)(A_C - A(x) - W\zeta(x)) \tag{5}$$

with

$$V_1(x) = V + \delta V(x) \tag{6}$$

Eq. (4) assumes that the free surface over the full width of the canal section sinks. Fig. 6 shows a level drop $\zeta(x)$, while the section of the vessel at this position x sinks over the same distance. This decrease of the water depth $\zeta(x)$ can be calculated with Bernoulli's Law:

$$\zeta(x) = \frac{1}{2g}(V_1(x)^2 - V^2) \tag{7}$$

The substitution of Eq. (4) into Eq. (6) results in:

$$\frac{1}{2g}(V_1(x)^2 - V^2) = \frac{A_C}{W} - \frac{A(x)}{W} - \frac{A_C}{W}\frac{V}{V_1(x)} \tag{8}$$

Because of the rectangular cross section of the fairway A_C/W equals the initial water depth h and $A(x)/A_C$ is known as the blockage ratio m, Eq. (7) can now be written as:

$$\frac{1}{2}\frac{V^2}{gh}\left(\left(\frac{V_1(x)}{V}\right)^2 - 1\right) + \frac{V}{V_1(x)} + m(x) - 1 = 0 \tag{9}$$

Substituting the water depth dependent Froude number Fr_h from Eq. (2) and multiplying by $V_1(x)/V$ in Eq. (9).

$$\frac{1}{2}Fr_h^2\left(\frac{V_1(x)}{V}\right)^3 - \left(\frac{1}{2}Fr_h^2 + 1 - m(x)\right)\frac{V_1(x)}{V} + 1 = 0 \tag{10}$$

Eq. (9) has always three solutions for $V_1(x)$. One solution is always real and negative, and has no physical meaning. When the blockage factor m is less than a critical blockage factor m_{crit}, both remaining solutions are real and positive; for greater values of m these solutions are complex conjugated numbers which means that no stationary solution can be found. For a given value of the depth Froude number, the critical value of the blockage factor is given by:

$$m_{crit} = 1 - \sin\left(3\arcsin\left(\frac{Fr_h^{2/3}}{2}\right)\right) \tag{11}$$

This equation is valid if $Fr_h < 1$, as was shown by Schijf (1949), see also Briggs et al. (2010).

For a given value of the blockage factor m, a physically realistic solution is only possible if Fr_h is either less than a first critical value, or greater than a second critical value. In this way, subcritical, transcritical and supercritical speed ranges can be distinguished. In the transcritical speed range, which always contains $Fr_h = 1$, no stationary solution can be found.

The first critical depth Froude number is always less than 1 and can be calculated as follows as was shown by Schijf (1949) and more recently by Briggs et al. (2010):

$$Fr_{h,crit1} = \left(2\sin\left(\frac{\arcsin(1-m)}{3}\right)\right)^{3/2} \tag{12}$$

The second critical Froude number equals:

$$Fr_{h,crit2} = \left(2\sin\left(\frac{\pi - \arcsin(1-m)}{3}\right)\right)^{3/2} \tag{13}$$

Because of a physical maximum blockage factor of one the second critical Froude number $Fr_{h,crit2}$ is limited to $3^{3/4}$. In the subcritical speed range, the critical blockage m_{crit} decreases for an increasing Froude number Fr_h. For example, for a blockage m of 0.01 the critical Froude number $Fr_{h,crit}$ decreases from 1.0 to 0.88. The subcritical area in Fig. 7 indicates the combinations of the depth Froude number and the blockage factor for which a valid physical real solution for Eq. (9) exists. An equilibrium is reached by a water level decrease because the velocity V_1 at the cross section is higher than the undisturbed velocity V.

At a (high) ship's speed V the velocity V_1 cannot increase further and the water in front of the vessel accumulates and induces a pressure wave. This pressure wave travels at a higher speed than the vessel. This causes an increasing water level ζ in front of the vessel. Because of this high water volume in front of the vessel, a decrease of the water level occurs at the stern as not enough water can flow to the back of the vessel (Fig. 8). In this transcritical speed range a stationary equilibrium is not reached.

When the ship sails at a speed higher than the critical speed (supercritical speed range) the velocity V_1 will be lower than the forward speed of the vessel V and a new equilibrium will be

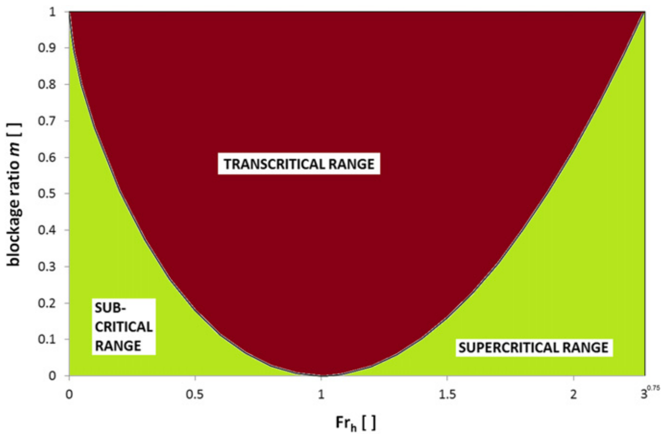

Fig. 7. A graphical interpretation of the solution areas for Fr_h and blockage ratio m.

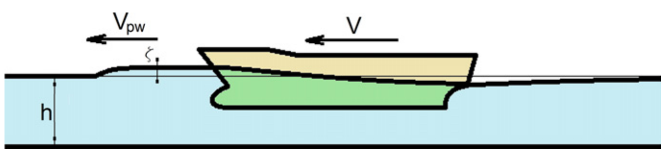

Fig. 8. The accumulation of the water in front of the vessel at transcritical forward speeds.

reached when the forward speed of the pressure wave V_{PW} equals the forward speed of the vessel. This paper, however, focuses only on the subcritical speed range.

When Eq. (9) is solved for $V_1(x)/V$, the local speed difference δV can be calculated for each longitudinal position x along the vessel. With this speed difference the local water level decrease $\zeta(x)$ and the local pressure drop $\rho g\zeta(x)$ are known. The integration of the pressure drop over the entire hull results in a vertical force Z and trim moment M.

$$Z=\rho g\int_{x_a}^{x_f}\zeta(x)B(x)dx \tag{14}$$

$$M=\rho g\int_{x_a}^{x_f}\zeta(x)B(x)xdx \tag{15}$$

The vertical force Z and trim moment M equal the hydrostatic force and moment:

$$Z=\rho gA_W z_{VM} \tag{16}$$

$$M=\rho gI_L t_M \tag{17}$$

This results in a running trim and mean sinkage of the vessel:

$$z_{VM}=\frac{\int_{x_a}^{x_f}\zeta(x)B(x)dx}{\int_{x_a}^{x_f}B(x)dx} \tag{18}$$

$$t_M=\frac{\int_{x_a}^{x_f}\zeta(x)B(x)xdx}{\int_{x_a}^{x_f}B(x)x^2dx} \tag{19}$$

The running sinkage at the FP (forward perpendicular) z_{VF} and at the AP (aft perpendicular) z_{VA} can now be calculated:

$$z_{VF}=z_{VM}-\frac{Lpp}{2}t_M \tag{20}$$

$$z_{VA}=z_{VM}+\frac{Lpp}{2}t_M \tag{21}$$

The trim and sinkage of the vessel (or the changing water level) will change the cross section $A_C(x,\zeta)$ and the blockage ratio. An iteration can be started to calculate the new trim and sinkage

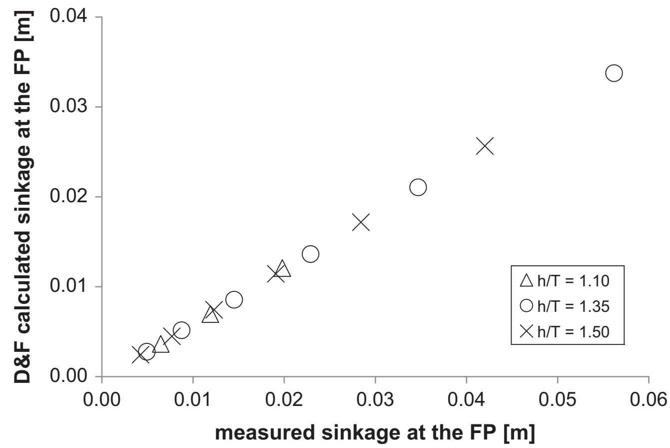

Fig. 9. The measured and calculated running sinkage at the FP on the centreline of a five beams wide channel, at all speeds and water depths tested.

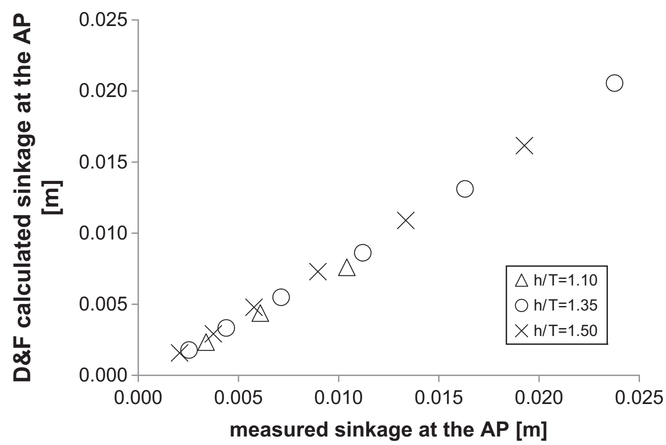

Fig. 10. The measured and calculated running sinkage at the AP on the centreline of a five beams wide channel, at all speeds and water depths tested.

based upon this new cross section $A_C(x,\zeta)$ until a final equilibrium is reached. The final trim and sinkage, however, change little after the first iteration.

4.2. Comparison with model tests

The running sinkage at the FP (z_{VF}) and at the AP (z_{VA}) determined with the D&F-method can now be compared with the measurements of the squat when the ship model was towed at the centreline of the installed fairway. As an example, in Fig. 9 and Fig. 10 the values of the running sinkage at the FP and at the AP, respectively, during model tests performed in a rectangular canal with a width $W=5.0\,B$ are plotted versus the sinkage values calculated with the D&F-method, for all tested underkeel clearances and forward speeds. Although a strong correlation (Table 5) between the calculated and measured sinkage is found for this particular fairway, a large absolute deviation between calculated and measured values is observed. The influence of water depth and forward speed was minimal on the ratio between the values calculated with the D&F-method and the measured sinkage at the FP or AP (e.g., Figs. 9 and 10).

The ratio between the measured running sinkage and calculated running sinkage appears to be different for each width of the test section. In Figs. 11 and 12 this ratio (and deviation) is plotted versus the ratio of the ship's beam and width of the test section. The correlation for the sinkage at the FP is almost linear

Table 5
Coefficient of determination for the sinkage D&F/measured at the FP and AP.

	Canal width *W*					
	1.05 *B*	**1.25 *B***	**1.70 *B***	**2.50 *B***	**5.00 *B***	**9.05 *B***
Coefficient of determination R^2 for sinkage at the FP D&F/measured	0.9188	0.9556	0.9415	0.9991	0.9996	0.9989
Coefficient of determination R^2 for sinkage at the AP D&F/measured	0.8925	0.9809	0.9434	0.9947	0.9923	0.9763

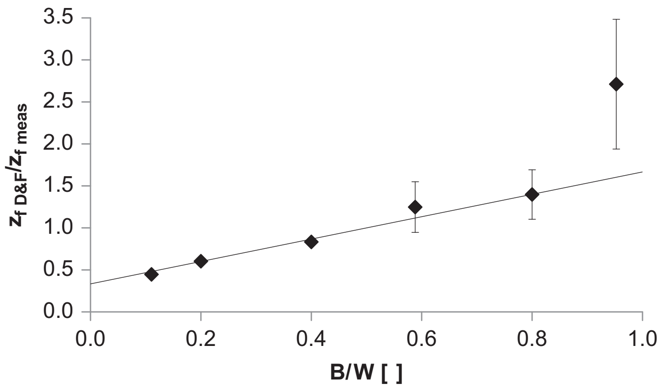

Fig. 11. Ratio between the calculated and measured values of the sinkage at the FP as a function of the ratio of the ship's beam and canal width and the confidence interval (95%).

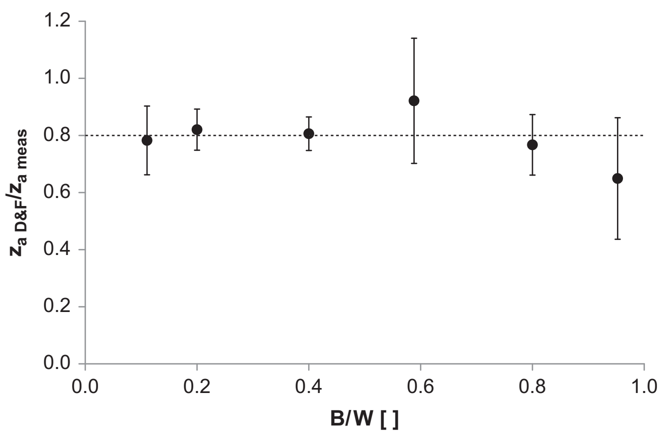

Fig. 12. Ratio between the calculated and measured values of sinkage at the AP as a function of the ratio of the ship's beam and canal width and the confidence interval (95%).

(coefficient of determination $R^2 = 0.977$) for that B/W ratio except for the extremely narrow test section. For a test section of 1.70 times the beam of the ship, the D&F-method and measurements for the sinkage at the FP almost coincide. When the test section is narrower, the D&F-method overestimates the sinkage. A plausible explanation for this phenomenon is the following. Because the test section is open at the outlet the vessel is able to act as a piston and pushes water out of the test section; in this way, not all the displaced water has to flow around the vessel, resulting in a measured sinkage which is lower than the calculated sinkage. For cross sections wider than about 1.70 times the ship's beam, the measured sinkage at the FP appears to be higher than the calculated value. Again this D&F-method supposes that the decrease of the water level is constant over the entire cross section. This is not the case in a wider channel where the water level will decrease more in the vicinity of the vessel than further away. The vessel acts as if it were sailing in a smaller cross section.

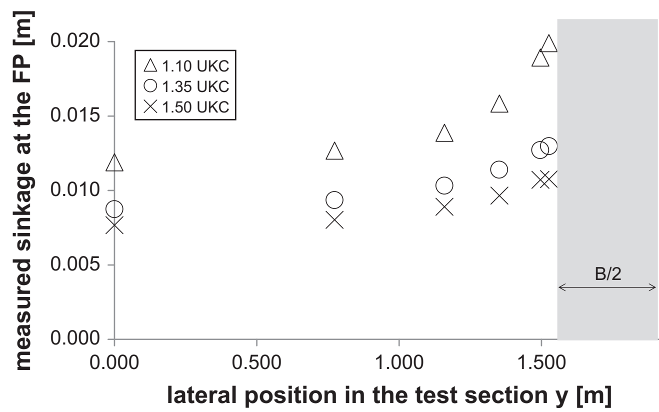

Fig. 13. The measured running sinkage at the FP for a wide range of lateral positions in a canal width of 5 *B* and at 8.0 knots full scale.

For the running sinkage at the AP (Fig. 12) this ratio takes an almost constant value of approximately 0.80 which implies that the measured sinkage at the AP was always about 25% higher than the sinkage at the AP calculated with the D&F-method. Remark that the coefficient of determination is for most canal widths lower than it is for the sinkage at the FP (Table 5).

The model tests were executed systematically for a wide range of lateral positions in the test section: during the test program, the closest distance between the ship's side and the bank was varied between twice the ship's beam (i.e., at the centreline of the five ship beams wide channel) and 20 mm (1.50 m full scale) for the $(W/B) = 1.05$ case. In Fig. 13 the sinkage at the FP is shown as a function of the lateral position in the test section for the three tested water depths. The running sinkage at the FP increases with decreasing distance to the vertical wall. The influence of this eccentricity cannot be neglected and will be captured in the newly proposed mathematical model.

Because the D&F-method does not result in an accurate absolute prediction of the sinkage at the FP and AP, and also the influence of the lateral position of the vessel in the fairway nor the propeller action were taken into account; a new mathematical model that addresses these shortcomings is proposed.

5. New mathematical model

5.1. Running sinkage at the FP z_{VF}

Based upon the measured running sinkage at the FP z_{VF} and the D&F-method for every ship speed, eccentricity y and water depth h, a new width can be calculated which results in the same running sinkage at the FP as the measured running sinkage during the model tests. This results in an equivalent width W_{eq} based upon the measured sinkage at the FP z_{VF}. As discussed in Section 4, this new canal width W_{eq} is smaller than the real canal width when the canal is wider than about 1.7 the ship's beam and vice versa. The influence of the eccentricity y also differs for different canal widths but remains consistent with $|((1/2)B/(1/2)W-y) -((1/2)B/(1/2)W+y)|$ for all speeds and water depths.

A function dependent on the original canal width W and eccentricity y that results in an accurate prediction of the equivalent width W_{eq} can be derived. The model will be split into a part that takes into account the total width of the cross section (W_0), and a part that takes into account the influence of the eccentric position in the rectangular canal (W_y):

$$W_{eq}(W,y) = W_0 + W_y \tag{22}$$

For ships navigating in the centreline of the rectangular canal, the following expression appears to give acceptable results:

$$W_0 = W\frac{\xi_1 B}{\xi_2 B + W} \tag{23}$$

which implies that the equivalent width W_0 is greater than the actual width W for $W/B > \xi_1 - \xi_2 = 1.80 \pm 0.25$.

The contribution of eccentricity to the equivalent width is expressed by:

$$W_y = W\left(\xi_3\frac{\xi_1 B}{\xi_2 B + W} + \xi_4\right)\left|\frac{\frac{B}{2}}{\frac{W}{2}-y} - \frac{\frac{B}{2}}{\frac{W}{2}+y}\right| \tag{24}$$

or

$$W_y = W\left(\xi_3\frac{W_0}{W} + \xi_4\right)\left|\frac{B}{W-2y} - \frac{B}{W+2y}\right| \tag{25}$$

The last factor in Eqs. (23) and (24) takes a value between 0 and 1, the latter occurring if the ship sails with zero lateral clearance in an infinitely wide canal and 0 when the ship sails on the centreline ($y=0$). For the range of W/B values considered in the test program (1.05–9.05), the maximum values of the factor within the absolute value marks are physically limited to a value between 0.375 for the narrowest canal and 0.94 for the widest canal. As the sinkage increases due to eccentricity, W_y is expected to be negative.

Based upon the results of all model tests, but excluding the tests at a canal with width 1.05 B, the ξ-values listed in Table 6 were obtained.

This new proposed canal width W_{eq} can be used as input to recalculate the sinkage at the FP with the D&F-method. Fig. 14 is similar to Fig. 13 for the sinkage at the FP, but also includes the new calculated sinkage at the FP (with W_{eq}) that includes the relative lateral position effects ($W_y \neq 0$).

Fig. 15 shows the measured sinkage at the FP versus the new calculated running sinkage. A satisfying correlation ($R^2=0.965$) is found. It should be taken into account that the range of the canal width is very extreme from more than 9 times the ship's beam up to only 1.05 times the ship's beam (similar as in the current Panama locks). Some of the discrepancies occur at this smallest canal width because the regression model does not take account of the experiments carried out in this canal.

Table 6
Regression results for the equivalent width.

Coefficient	Value	Std. error	95% Confidence interval	
			Lower bound	Upper bound
ξ_1	8.260	0.134	7.997	8.524
ξ_2	6.458	0.211	6.043	6.873
ξ_3	0.151	0.075	0.004	0.298
ξ_4	−0.317	0.051	−0.418	−0.216

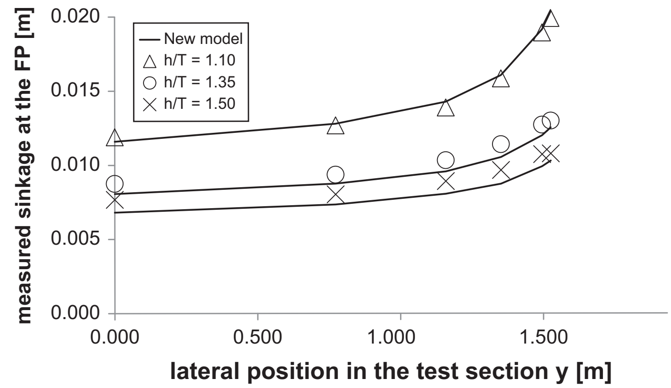

Fig. 14. The measured and the modelled running sinkage at the FP for a range of lateral positions in a canal width of 5 B and at 8.0 knots full scale.

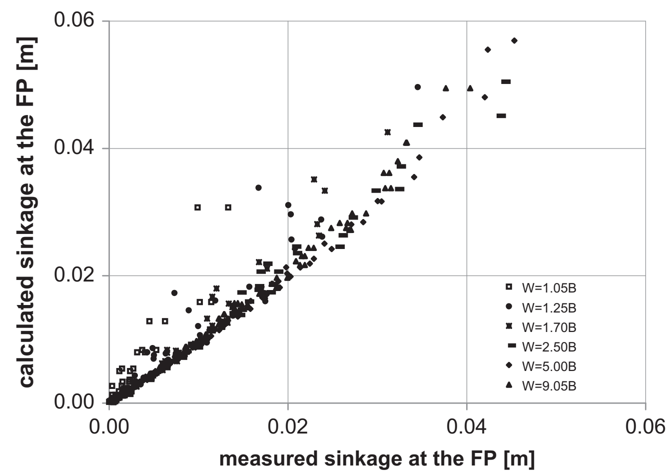

Fig. 15. The measured sinkage at the FP vs. the calculated sinkage based upon the newly proposed model with the equivalent width W_{eq}.

5.2. Running sinkage at the AP z_{VA}

The trim according to D&F does not correspond with the trim measured during the model tests. Since the ratio z_{VF}/z_{VA} with the D&F-method is almost constant, no combination of width of the canal and forward speed can be found with a similar running sinkage and trim combination as measured during the model tests. Therefore, an equivalent width is sought based on the running sinkage at the FP z_{VF} that can be used subsequently with a new forward speed V_{eq} that produces the same running sinkage at the AP z_{VA} as measured during the model tests.

Only during model tests in the widest channel ($W=9.05$ B) was the ship model systematically tested with a propeller rate according to self propulsion in open water (at each tested speed) and with a fixed propeller (propeller rate = 0 rpm). Fig. 16 presents the measured sinkage at the FP with a fixed propeller versus the measured sinkage at the FP with a propeller with self propulsion. All points are very close to the first bisector (dotted line in Fig. 16) indicating a negligible influence of the propeller action on the sinkage at the FP. Fig. 17 presents similar results for the sinkage at the AP. As expected, the propeller rate has an increasing effect on the running sinkage at the AP.

To take the effect of the propulsion into account in the mathematical model, the speed V_T is introduced based upon the propeller thrust and propeller diameter. This speed represents in a simplified way the axial speed in the flow field behind the propeller induced by the propeller. The flow around the stern will

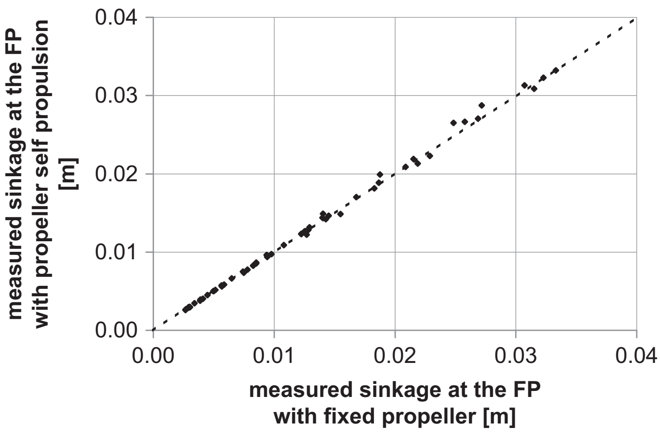

Fig. 16. The sinkage at the FP with a fixed propeller versus the sinkage at the FP with the same test parameters but with the propeller rate according to open water self propulsion for all tested speeds, water depths and lateral positions in a canal section of 9.05 *B* wide.

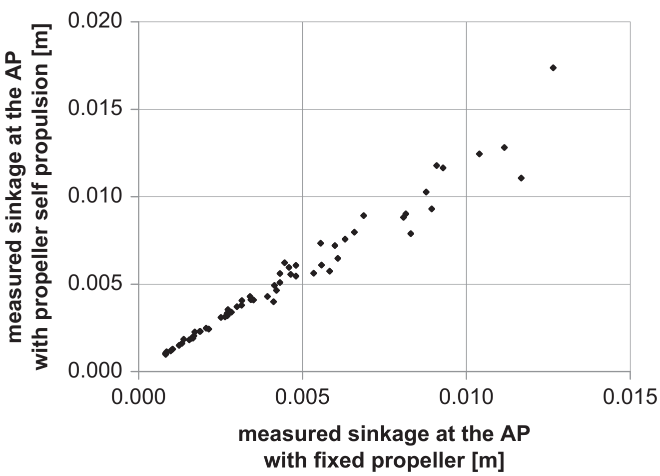

Fig. 17. The sinkage at the AP with a fixed propeller versus the sinkage at the AP with the same test parameters but with the propeller rate according to open water self propulsion for all tested speeds, water depths and lateral positions in a canal section of 9.05 *B* wide.

increase due to the forward propeller action and will decrease when the propeller is fixed. A fraction of the speed V_T is added (or subtracted) to (from) the forward speed of the vessel to take into account this propeller effect.

$$V_T = \mathrm{sign}(T_P)\sqrt{\left|\frac{8T_P}{\rho\pi D^2}\right|} \tag{26}$$

$$V_{eq} = V + \xi_5 V_T \tag{27}$$

Based upon the sinkage at the AP, the equivalent speed can be calculated as in eq. (27) with the forward speed of the vessel V, width of the fairway W, V_T and beam of the vessel as variables.

$$V_{eq}(B,V,V_T,W) = (V+\xi_5 V_T)\left(\xi_6 \frac{B}{W}+\xi_7\right) \tag{28}$$

The following ξ-values are determined with the measured sinkage at the AP during the model tests, but excluding the tests at a canal with width 1.05 *B* (Table 7)

With the equivalent width W_{eq}, defined in Eq. (22), and the equivalent speed V_{eq} as input for the D&F-method, the sinkage at the AP can be calculated. Fig. 18 plots the running sinkage at the AP with this method and the measured sinkage at the AP. The correlation is satisfactory ($R^2 = 0.974$), except for the smallest canal widths, which were excluded from the regression analysis.

Table 7
Regression results for the equivalent speed.

Coefficient	Value	Std. error	95% Confidence interval	
			Lower bound	Upper bound
ξ_5	0.053	0.009	0.036	0.070
ξ_6	0.603	0.022	0.561	0.646
ξ_7	0.696	0.008	0.680	0.712

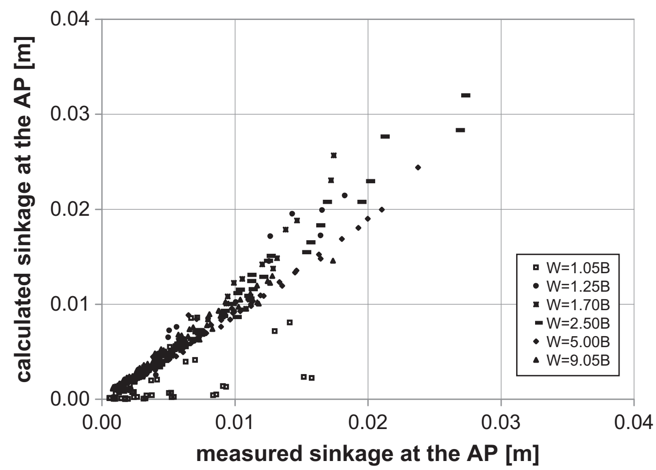

Fig. 18. The measured sinkage at the AP vs. the calculated sinkage based upon the newly proposed model with the equivalent width W_{eq} and forward speed V_{eq}.

6. Future research opportunities

The newly proposed mathematical model will be validated against the sinkage of other ship types. The independence of the coefficients relative to the ship's geometry will also be tested. The cross section of a natural river or a manmade canal is seldom rectangular, therefore other cross sections than rectangular cross sections of the fairway will be investigated. As a consequence a new formulation for the influence of the lateral position of the vessel on the equivalent width will be inevitable. Since this squat model can cope with high blockage ratios, it might be useful to investigate the hydrodynamics when sailing into or out of a lock. However, during this research project the inlet and outlet of the test section was always open, which can cause an important difference between these tests and a real lock.

7. Conclusions

Model tests have been carried out with a scale model of a very large crude carrier in canals of different widths. The sinkage of the ship has been measured at FP and AP and the measurements were compared with the empirical model determined by Dand and Ferguson (D&F).

The original D&F method for the sinkage at the FP corresponds to the measurements when $W \approx 1.8\ B$. When the section is wider the original D&F method underestimates the sinkage at the FP, while an overestimation is found when the section is smaller. Overall the original D&F method underestimates the running sinkage at the AP within 25% and could not take account of the effect eccentric sailing has on the running sinkage.

A new mathematical model was introduced based on an equivalent width that provides a better input for the D&F method. The sinkage at the FP and at the AP of a vessel sailing in a rectangular fairway parallel to the wall at any depth, width, subcritical speed, lateral position and propeller rate can then be determined with seven coefficients (Tables 6 and 7). The mathematical model takes account of the magnitude and distribution of the cross-sectional areas of the vessel as well as the longitudinal distribution of the beam on the water line of the vessel. The fairway can vary from an infinite open ocean (water depth and width infinite) to an extremely restricted canal in width and water depth with a rectangular cross section. In the near future the model will be validated against non-rectangular cross sections and other ship types.

Acknowledgments

This research project was funded by the Flemish Government, Department Mobility and Public Works, and the model tests were executed in 2010 by Flanders Hydraulics Research (Antwerp, Belgium). The presented research is executed in the frame of the Knowledge Centre Ship Manoeuvring in Shallow and Confined Water, a cooperation between Flanders Hydraulics Research and the Maritime Technology Division of Ghent University.

References

Ankudinov, V., Daggett, L., Hewlett, J., Jakobsen, B. 2000. Prototype measurement of ship sinkage in confined water. Proceedings of MARSIM 2000 (International Conference on Marine Simulation and Manoeuvrability), Orlando, USA, p. 233.
Barrass, C.B., 1979. The phenomena of ship squat. Int. Shipbuild. Prog. 26, 44–47.
Beck, R., Newman, J., Tuck, E., 1975. Hydrodynamic forces on ships in dredged channels. J. Ship Res. 19 (3), 166–171.
Blaauw, H., Van der Knaap, F., 1983. Prediction of squat of ships sailing in restricted water. Int. Harbour Congr., 81–93.
Briggs, M., Vantorre, M., Uliczka, K., Debaillon, P., 2010. Prediction of squat for underkeel clearance. In: Young, C Kim (Ed.), Handbook of Coastal and Ocean Engineering. World Scientific Publishing Company, pp. 723–774, chapter 26.
Brossard, C., Delouis, A., Galichon, P., Granboulan, J., Monadier, P. 1990. Navigability in channels subject to siltation. Proceedings of the 22nd International Coastal Engineering Conference, Delft, The Netherlands, pp. 3088–3101.
Cong, L., Hsiung, C., 1991. Computing wave resistance, wave profile and sinkage and trim of transom stern ships. Mar. Offshore Oper., 99–112.
Constantine, T., 1960. The Behaviour of Ships Moving in Restricted Waterways, University of Manchester, Paper no. 6499.
Dand, I. 1972. On Full form Ships in Shallow Water: Some Methods for the Prediction of Squat in Subcritical Flows. National Physical Laboratory, Ship Division, Ship Report 160.
Dand, I.W., Ferguson, A.M., 1973. Estimating the bow and stern sinkage of a ship under way in shallow water. Naval Architect 1973, 238.
de Koning Gans, H., Boonstra, H. 2007. Squat effects of very large container ships with drift in a harbor environment. Proceedings of the International Maritime-port Technology and Development Conference, Singapore, pp. 613–620.
Delefortrie, G., Vantorre, M., Eloot, K., Verwilligen, J., Lataire, E., 2010. Squat prediction in muddy navigation areas. Ocean Eng., 1464–1476.
Doctors, L.J., Zilman, G., Miloh, T., 1996. The influence of a bottom mud layer on the steady-state hydrodynamics of marine vehicles. 21st Symp. Naval Hydrodyn., 727–742.
Dumas, R., 1982. Le surenfoncement des navires dû à leur mouvement. Revue technique du service des phares et balises 53, 26–58.
Eloot, K., Verwilligen, J., Vantorre, M. 2008. An overview of squat measurements for container ships in restricted water. In: Varyani, K.S. (Ed.), International Conference on Safety and Operations in Canals and Waterways SOCW 2008, 15-16 September 2008, Glasgow, UK, pp. 106–116.
Führer, M., Römisch, K., 1977. Effects of modern ship traffic on inland- and ocean waterways and their structures, PIANC, 23, SI-3, Leningrad. USSR, 79–93.
Gourlay, T., 1999. The effect of squat on steady nonlinear hydraulic flow past a ship in a channel, Schiffstechnik Bd. 46. Ship Technol. Res. 46, 1999.
Gourlay, T. 2000. Mathematical and Computational Techniques for Predicting the Squat of Ships. Ph.D. Thesis. University of Adelaide, Department of Applied Mathematics.
Gourlay, T., 2008. Slender-body methods for predicting ship squat. Ocean Eng. 35 (2), 191–200.
Guliev, U.M., 1971. Calculs rélatifs au déjaugeage de navires qui naviguent dans des eaux peu profondes et dans des chenaux. P.I.A.N.C. Bull. I (7).
Härting, A., Laupichler, A., Reinking, J., 2009. Considerations on the squat of unevenly trimmed ships. Ocean Eng. 36, 193–201.
Härting, A., Reinking, J. 2002. SHIPS: a new method for efficient full-scale ship squat determination. PIANC 30th International Navigation Congress, Sydney, Australia, p. 84-91.
Jiang, T., Henn, R. 2003. Numerical prediction of ship's squat and trim in shallow water. Proceedings of MARSIM 2003 (International Conference on Marine Simulation and Manoeuvrability), Kanazawa, Japan.
Martin, H., Puls, D., 1986. Vertical forces, trim moments and changes of draught and trim of ships in shallow water. Schiffbauforschung 25 (3), 155–159.
Millward, A., 1990. A preliminary design method for the prediction of squat in shallow water. Mar. Technol. 27 (1), 10–19.
Naghdi, P., Rubin, M., 1984. On the squat of a ship. J. Ship Res. 28 (2), 107–117.
PIANC 1997. Approach Channels — A Guide for Design. Final Report of the Joint Working Group PIANC and IAPH, in Cooperation with IMPA and IALA. Supplement to PIANC Bulletin, no. 95, p. 108.
Schijf, J.B., XVIIth International Navigation Congress Lisbon 1949 Section I Inland Navigation, pp. 61–78.
Sellmeijer, R., van Oortmerssen, G. 1983. The Effect of Mud on Tanker Manoeuvres. The Royal Institution of Naval Architects, Spring Meetings 1983, Paper no. 7.
Seren, D., Ferguson, A., McGregor, R., 1983. Squat — an examination of two practical prediction methods. Naval Architect 5, 228–230.
SIMMAN 2008, Workshop on Verification and Validation of Ship Manoeuvring Simulation Methods, Copenhagen, Denmark, April 14th-16th 2008.
Stern, F., Agdrup, K. (Ed.) (2008). SIMMAN 2008. Workshop on Verification and Validation of Ship Manoeuvring Simulation Methods, Copenhagen, April 14th— 16th 2008: Preprints of Workshop Proceedings: Volume 1. Summary, Test Cases, Methods and Papers. Force Technology: Brøndby. Different Pagination.
Stocks, D., Daggett, L., Page, Y. 2004 Maximization of Ship Draft in the St.-Lawrence Seaway. Squat Workshop 2004, Elsfleth, Germany.
Tuck, E., 1966. Shallow water flow past slender bodies. J. Fluid Mech. 26 (1), 81–95.
Tuck, E., 1967. Sinkage and trim in shallow water of finite width. Schiffstechnik 14 (73), 92–94.
Van Kerkhove, G., Vantorre, M., Delefortrie, G. 2009, Advanced model testing techniques for ship behaviour in shallow and confined water. Proceedings of AMT 2009 (The 1st International Conference on Advanced Model Measurement Technology for the EU Maritime Industry), Nantes, France, pp. 158–172.
Vantorre, M., Coen, I. 1988. On sinkage and trim of vessels navigating above a mud layer. The Royal Society of Flemish Engineers, International Harbour Congress.
Von Bovet, G., 1985. Tiefgangs- un Trimmwinkeländerungen von Schiffen under berücksichtigung endlicher Wassertiefe un Einfluβ auf die Steuerbarkeit. Schiffbauforschung 24 (1), 3–11.